Bioelectrochemical Systems and Applications
https://www.sciltp.com/journals/bsa

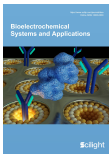

Article

Dual-Mode Lateral Flow Strip with Förster Resonance Energy Transfer for Rapid and Accurate Thrombin Detection

Qi Chen [1], Li Yao [1,2], Wei Qu [1], Haoyang Xu [1], Chao Yan [1], Jianguo Xu [1,3] and Wei Chen [1,4,*]

[1] Engineering Research Center of Bio-Process, MOE, School of Food and Biological Engineering, Hefei University of Technology, Hefei 230009, China
[2] School of Food Science and Bioengineering, Changsha University of Science & Technology, Changsha 410114, China
[3] College of Biological Chemical Science & Engineering, Jiaxing University, Jiaxing 314001, China
[4] Intelligent Manufacturing Institute, Hefei University of Technology, Hefei 230009, China
* Correspondence: chenweishnu@163.com

How To Cite: Chen, Q.; Yao, L.; Qu, W.; et al. Dual-Mode Lateral Flow Strip with Förster Resonance Energy Transfer for Rapid and Accurate Thrombin Detection. *Bioelectrochemical Systems and Applications* **2025**, *1*(1), 2.

Received: 9 March 2025
Revised: 27 June 2025
Accepted: 1 July 2025
Published: 15 July 2025

Abstract: Thrombin, a serine protease, is a critical biomarker for blood-related diseases, with its serum levels playing a key role in clinical diagnosis. In this study, we developed a dual-aptamer-based, dual-mode Förster resonance energy transfer (FRET) lateral flow strip for the rapid and sensitive detection of thrombin. Quantum dots (QDs) were employed as the energy donor, while gold nanoparticles (AuNPs) served as the acceptor. Upon thrombin binding, the colorimetric signal from AuNPs and the fluorescent signal from QDs exhibited distinct variations, each acting as an independent indicator for precise quantification. Using this dual-mode FRET lateral flow strip, thrombin was successfully detected in serum samples, achieving a fluorescence-based detection limit of 0.135 nM-twice as sensitive as the colorimetric method. The integration of FRET and lateral flow strip technologies provides a robust platform for precise biomarker detection and significantly enhances the performance of colorimetric assays.

Keywords: dual-aptamer; Förster resonance energy transfer (FRET); lateral flow strip; thrombin; dual-mode

1. Introduction

Thrombin, a member of the serine protease family, plays a pivotal role in various pathological processes [1]. It activates platelets, converts soluble fibrinogen into fibrin, and promotes hemostasis and coagulation, thereby facilitating vascular and tissue repair while accelerating wound healing [2–4]. Additionally, thrombin acts as a key enzyme in several biological processes, including innate immunity, embryonic development, angiogenesis, neurodegeneration, inflammation, tumor growth, and metastasis [4–9]. It is also implicated in diseases such as thrombosis, Alzheimer's disease, and atherosclerosis [4,10–12]. Studies have shown that while low thrombin concentrations exert protective effects on cells, elevated levels can lead to kidney damage [13,14]. Therefore, the development of highly sensitive and accurate thrombin detection methods is crucial for disease diagnosis and drug evaluation.

In recent decades, advancements in the rapid detection technologies of biomarkers for serum and other biological fluids have garnered significant attention in biomedical diagnostics [15–18]. Among these innovations, immunochromatographic lateral flow technology has become a widely adopted method for on-site screening and diagnosis. The lateral flow strip (LFS) is recognized as one of the most advanced point-of-care testing (POCT) technologies, as it meets the ASSURED criteria and plays a crucial role in rapid analyte detection [19–22]. Currently, most LFS assays rely on single-mode signal output [23,24]. At high analyte concentrations, targets can be visually detected with the naked eye. However, at lower concentrations, visual detection may be unreliable due

to subtle color variations on the test (T) line caused by single-mode detection, leading to signal instability. Most existing LFS systems rely on single-signal intensity or brightness responses, making them vulnerable to environmental factors and non-specific interferences, which can cause signal fluctuations or detection failures [25,26]. Therefore, enhancing the sensitivity and stability of LFS, particularly for the reliable detection of low-concentration analytes, remains a critical challenge in the field.

To address these limitations, dual-mode detection platforms integrating both colorimetric and fluorescent signals have gained increasing attention [27,28]. The combination of these distinct yet complementary modalities enable rapid visual screening and simultaneous quantitative fluorescence measurement for precise analyte determination. This dual-signal approach enhances detection robustness, expands the dynamic range, and reduces the likelihood of false negatives due to ambiguous signals or environmental interference. Thus, dual-mode detection systems offer a more comprehensive and reliable solution for diagnostic applications that demand both intuitive visualization and high analytical performance.

To meet the demand for enhanced sensitivity and dual-mode capability, FRET technology has been proposed. Due to its strong resistance to background fluorescence and environmental interference, FRET has become a widely used technique in fluorescence detection and a crucial tool for precise quantitative analysis [29,30].

A key challenge in developing FRET-based platforms is the design of donor-acceptor pairs and the enhancement of FRET efficiency. QDs are an exceptional class of fluorescent materials with particle sizes ranging from 1 to 10 nm. They exhibit unique optical and electronic properties, including a broad excitation spectrum and precisely tunable, symmetric emission spectra [31]. Additionally, QDs demonstrate remarkable resistance to photobleaching and exceptional photostability, making them highly efficient fluorescent donors [32]. Currently, AuNPs [33], silver nanoparticles (AgNPs) [34], and polydopamine nanospheres (PDANs) [35] are widely employed in biosensors as fluorescence quenchers. Among these, AuNPs offer distinct advantages due to their simple synthesis process, high stability, excellent reproducibility, and strong resistance to background interference, along with superior fluorescence quenching capability. Therefore, AuNPs and QDs are among the most promising quenchers and fluorescent donors for developing dual-mode lateral flow strip assays to enhance detection performance.

In this study, we developed a dual-mode FRET-based lateral flow strip platform for the rapid detection of thrombin in serum samples, using dual aptamers as recognition probes. In the presence of thrombin, AuNPs act as acceptors, while QDs serve as donors, forming a sandwich structure on the test lines of a nitrocellulose (NC) membrane through specific aptamer-thrombin interactions. The FRET efficiency is regulated by the thrombin concentration in the sample. This method is not only simple and rapid but also significantly enhances detection accuracy and sensitivity, providing an excellent alternative for detecting other biomarkers.

2. Materials and Methods

2.1. Chemicals and Materials

Selenium powder (99.8%), 3-mercaptopropionic acid (MPA, 99%), N-hydroxysuccinimide (NHS), 1-ethyl-3-(3-dimethylaminopropyl) carbodiimide hydrochloride (EDC), and chloroauric acid ($HAuCl_4$) were all purchased from J&K Chemical Scientific Ltd. (Shanghai, China). Streptavidin (SAV), trisodium citrate, deoxyadenosine triphosphate (dATP), sodium hydroxide (NaOH), sodium borohydride ($NaBH_4$), Tris (2-carboxyethyl) phosphine (TCEP), and cadmium chloride ($CdCl_2 \cdot 2.5H_2O$) (99.99%) were obtained from Sinopharm Chemical Reagent Co., Ltd. (Beijing, China). The conjugate pads, NC membrane, sample pad and absorbent pad for strip assembly were ordered from Whatman GmbH (Dassel, Germany). The thrombin standard sample was purchased from the J&K Scientific Ltd. (http://www.jkchemical.com/). All other solvents and reagents related to this experiment were of analytical grade and used as received from Sinopharm Chemical Reagent Co., Ltd. It is essential to emphasize that Millipore Milli-Q ultrapure (>18 MΩ) water was used throughout the research.

2.2. Oligonucleotide Probes

The thrombin-binding aptamers and the single-stranded DNA (ssDNA) probe for the control (C) line on the lateral flow strip were synthesized by Sangon Biotechnology Co., Ltd. (Shanghai, China). The sequences of the ssDNA probes are as follows: Aptamer 1, which recognizes thrombin and is labeled with AuNPs, 5′-thiol-GGT TGG TGT GGT TGG-3′; Aptamer 2, which binds thrombin and serves as the immobilization probe on the test (T) line, labeled with QDs, 5′-NH_2-AGT CCG TGG TAG GGC AGG TTG GGG TGA CT-biotin-3′; And the C-line ssDNA probe, 5′-biotin-ATT CCA ACC ACA CCA-3′.

2.3. Preparation of Carboxyl Functionalized CdSe QDs and QD-Aptamer 2 Conjugates

2.3.1. Preparation of the Precursor

The synthesis of CdSe QDs was adapted from previously established methods with minor modifications [36]. Selenium powder (0.241 g, 3.0 mmol) and $NaBH_4$ (0.189 g) were dissolved in 4.0 mL of ultrapure water to prepare the precursor solution for CdSe QD crystal growth, a crucial step in the QD synthesis process. The mixture was sealed in a container with a pinhole for ventilation to allow the formation of a transparent, homogeneous solution. The precursor solution was stored in the dark at 4 °C for 24 h before use.

2.3.2. Preparation of MPA-Stabilized CdSe QDs

MPA-stabilized CdSe QDs were synthesized as follows: $CdCl_2 \cdot 2.5H_2O$ (0.57 g) was dissolved in 148 mL of deionized water in a 250-mL three-neck flask under continuous stirring. Subsequently, 0.5 mL of MPA was added, and the pH of the solution was adjusted to 7.5 using 1.0 M NaOH. The flask was degassed with nitrogen for 30 min before rapidly injecting 1.2 mL of the prepared precursor solution, leading to a color change to light orange. The reaction mixture was then maintained under a constant nitrogen stream for an additional 10 to 20 min. Finally, the solution was transferred to a 100-mL autoclave and reacted under varying conditions to obtain water-soluble MPA-stabilized CdSe QDs of different sizes. The synthesized CdSe QDs were stored in the dark at 4 °C for future use. Fluorescence spectra of the QDs were recorded using an RF-5301PC spectrophotometer (Shimadzu, Japan) with excitation at 395 nm.

2.3.3. Preparation of QD-Aptamer 2 Conjugates

The synthesized water-soluble CdSe QDs were used as fluorescent labels and conjugated with aptamer 2 in an aqueous solution via a conventional EDC/NHS-mediated process. Specifically, the carboxyl groups on the QD surface were activated by adding 10 μL of 20 mg/mL EDC and 5 μL of 20 mg/mL NHS, followed by a 30-min reaction. Subsequently, 12.5 μL of 50 μM 5′-amino-functionalized aptamer 2 was added to react with the activated carboxyl groups on the QD surface. After 3 h of continuous vortexing in the dark, 12.5 μL of 5 mg/mL SAV was introduced into the reaction mixture and incubated for an additional 2 h under the same conditions.

2.4. Preparation of AuNPs and AuNP-Aptamer 1 Conjugates

AuNPs with an average diameter of 15 nm were synthesized using a classic chemical reduction method, as described in our previous work [37]. Briefly, 850 μL of 5 g/L $HAuCl_4$ solution was added to a 250-mL flask containing 50 mL of ultrapure water, which was then heated to boiling. Next, 1000 μL of a 1% sodium citrate solution was quickly injected into the boiling mixture at 1500 rpm. The color change from transparent to dark blue, and finally to wine red confirmed the successful synthesis of AuNPs. The mixture was boiled for an additional 5 min and then cooled to room temperature (RT). The synthesized AuNPs were stored at 4 °C for later use.

For conjugation, 15 μL of 10 μM thiol-modified aptamer 1 (the recognition probe) was activated with 4.0 μL of 1.0 mM TCEP in 3 μL of 0.5 M acetate buffer (pH 5.0) at RT for 1 h. After activation, 100 μL of 10-fold concentrated AuNPs was added to the solution, which was stirred for an additional hour at RT. Next, 20 μL of 10-mM dATP was introduced and allowed to react for 30 min to block the residual surface of the AuNPs, preventing non-specific adsorption. Finally, the AuNP-aptamer 1 conjugates were aged by adding 20 μL of 100 mM NaCl and incubating for another 30 min at RT. The conjugates were then further aged at 4 °C for 6 h. Purification was performed by centrifuging the conjugates at 9300× *g* for 7 min, after which the precipitate was resuspended in 100 μL of a suspension solution containing 20 mM Na_3PO_4, 5% BSA, 0.25% Tween-20, and 10% sucrose.

2.5. Construction of the Dual-Mode FRET Lateral Flow Strip

The FRET lateral flow strip comprises five key components: a sample pad, a conjugate pad, an NC membrane, an absorbent pad, and a plastic adhesive pad. During NC membrane preparation, QD-aptamer 2 conjugates (Section 2.3.3) are immobilized on the NC membrane as the T line via a biotin-streptavidin recognition system. Meanwhile, 2.5 μL of 100 μM ssDNA probe and 2.5 μL of 5 mg/mL SAV are incubated at RT for 2 h before being immobilized as the C line. The NC membrane is then incubated at 37 °C for 24 h. Similarly, AuNP-aptamer 1 conjugates (Section 2.4) are immobilized on the conjugate pad using the Biodot 3000 and incubated under the same conditions. During LFS assembly, each pad overlaps with the adjacent pad by 2 mm to ensure efficient fluid migration, as shown in Figure 1B.

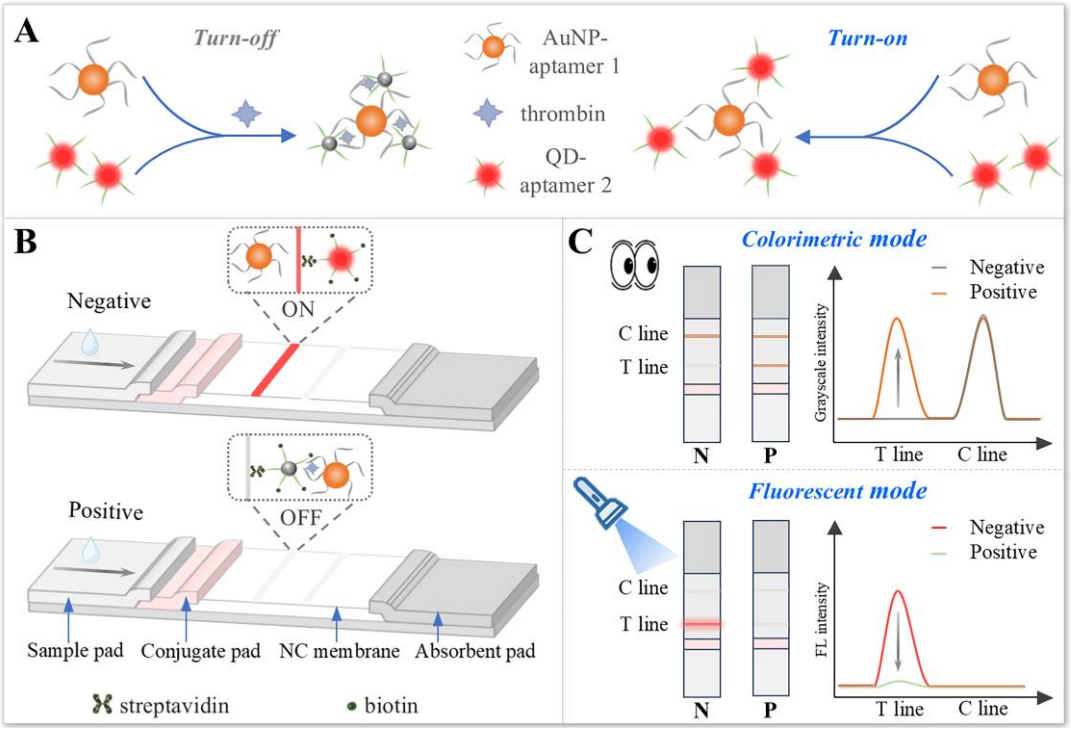

Figure 1. Schematic representation of the dual-mode FRET lateral flow strip for thrombin detection. (**A**) FRET mechanism: thrombin binding induces the formation of a QD–aptamer 2 (donor)/AuNP–aptamer 1 (acceptor) sandwich complex, resulting in fluorescence quenching. (**B**) Principle of thrombin detection using the FRET-based LFS. (**C**) Detection results under natural light and UV light.

2.6. Analytical Procedure for Thrombin Detection Using the Dual-Mode FRET Lateral Flow Strip

Thrombin samples with varying concentrations were prepared by diluting a standard thrombin solution in PBS (0.01 M, pH 7.4). For standard sensing procedures, 80 μL of thrombin solution at each concentration was applied to the sample pad of the lateral flow strip. After 10 min of reaction, both colorimetric and fluorescence signals were measured simultaneously, allowing for rapid qualitative and quantitative detection of thrombin. Quantitative analysis was conducted using ImageJ (http://imagej.nih.gov/ij). For real serum sample analysis, thrombin was spiked into blank human serum samples and detected using the developed dual-mode FRET lateral flow strip.

3. Results and Discussion

3.1. Principle of the Dual-Mode FRET Lateral Flow Strip for Thrombin Detection

The principle of the dual-mode FRET lateral flow strip for thrombin detection is illustrated in Figure 1. As shown in Figure 1A, the FRET system consists of QD-modified aptamer 2 (QD-aptamer 2) as the energy donor and AuNP-modified aptamer 1 (AuNP-aptamer 1) as the energy acceptor. The fluorescence signal alternates between “off” and “on” states depending on the presence of thrombin.

Figure 1B illustrates that the dual-mode FRET lateral flow strip operates based on the sandwich recognition principle, utilizing two thrombin-specific aptamers (aptamer 1 and aptamer 2). Specifically, AuNP-aptamer 1 is applied to the conjugate pad using a Biodot 3000, while QD-aptamer 2 is immobilized on the NC membrane at the T line via a biotin-streptavidin recognition system. In the absence of thrombin, the AuNP-aptamer 1 is not captured on the T line, resulting in no observable colorimetric signal. However, a strong fluorescent signal from the pre-immobilized QDs on the T line can be detected under 395 nm UV illumination. Conversely, in the presence of thrombin, specific interactions between aptamer 1, aptamer 2, and thrombin lead to the formation of a sandwich structure (AuNP-aptamer 1-thrombin-QD-aptamer 2) on the T line. This structure facilitates the formation of a classic FRET pair, in which the colorimetric signal from the AuNPs becomes visible, while the fluorescence of the QDs decreases due to the fluorescence quenching effect of the AuNPs. By integrating these dual signals—colorimetric and fluorescent—on the same T line, their opposite trends serve as indicators for qualitative and quantitative analysis.

Regardless of thrombin presence, the AuNP-aptamer 1 is captured on the C line of the lateral flow strip through hybridization with its complementary ssDNA probe, producing a colorimetric signal from the AuNPs. Figure 1C presents the visual and quantitative detection results of the dual-mode FRET lateral flow strip.

3.2. Analytical Performance of the Dual-Mode FRET Lateral Flow Strip for Thrombin Detection

Standard thrombin samples at varying concentrations (0, 0.135, 0.27, 0.54, 1.35, and 2.7 nM) were tested using the dual-mode FRET lateral flow strip, and the results were analyzed in both colorimetric and fluorescent modes. As shown in Figure 2A, the signal intensity on the T-line increased proportionally with thrombin concentration under natural light, with a detectable signal observed at 0.135 nM. Under UV illumination, the fluorescence signal on the T-line progressively decreased as thrombin concentration increased, with a noticeable reduction at 0.135 nM. At 0.54 nM, the fluorescence signal was completely quenched due to the accumulation of AuNPs on the T-line. Compared to the blank control, the greater accumulation of AuNPs on the T-line led to a more pronounced quenching of QD fluorescence, confirming the FRET mechanism between AuNPs and QDs in the dual-mode FRET lateral flow strip. On the C-line, only the colorimetric signal was observed under both modes, and its intensity remained unchanged regardless of thrombin concentration, confirming the reliability of the FRET lateral flow strip for thrombin detection. The visual detection limit for thrombin in both colorimetric and fluorescent modes was determined to be 0.135 nM.

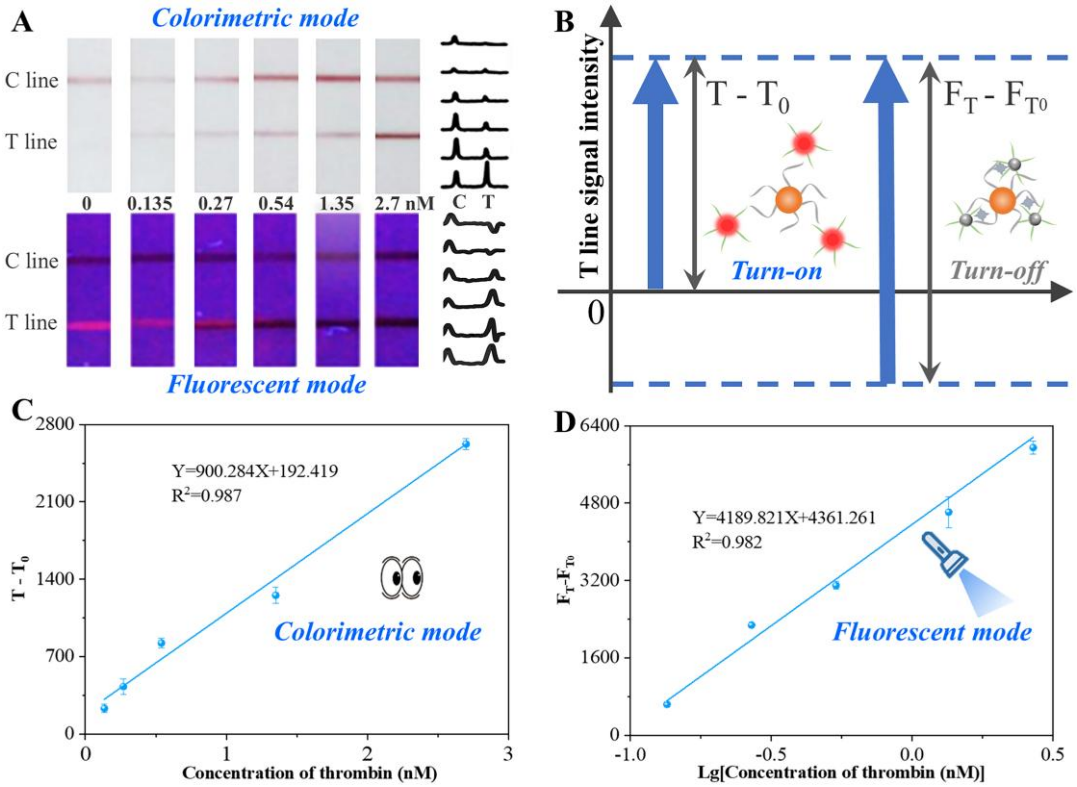

Figure 2. (**A**) Images of thrombin detection results in colorimetric and fluorescent modes, along with corresponding quantitative results analyzed using Image J (V. 1.8.0). (**B**) Variation in T-line signal under natural light and UV illumination. (**C**) Standard curve for thrombin quantification based on the relative intensity ($T-T_0$) in colorimetric mode. (**D**) Standard curve for thrombin quantification based on the relative intensity ($F_T-F_{T_0}$) in fluorescent mode.

To obtain quantitative results, Image J software was used to analyze images captured under both modes (Figure 2A). The peak intensity under natural light increased with thrombin concentration, while the initial fluorescence intensity under UV illumination was recorded as a negative value. As thrombin concentration increased, the fluorescence peak intensity shifted from a negative value to zero and then progressively increased into the positive range. Figure 2B illustrates the variations in colorimetric and fluorescence signals under natural light and UV illumination. Notably, fluorescence signal changes were more pronounced under UV illumination, indicating the stronger detection signal of the FRET lateral flow strip. Under UV illumination, fluorescence appeared as a bright signal, while AuNP-based colorimetric signals appeared as dark signals. This explains the negative fluorescence values observed at thrombin concentrations of 0 and 0.135 nM.

To evaluate the detection performance of the dual-mode FRET lateral flow strip, standard curves were generated for T-line intensity using Image J under both natural and UV light exposure, with thrombin concentrations ranging from 0 to 2.7 nM. The linear equation for the colorimetric mode was $Y = 900.284X + 192.419$ ($R^2 = 0.987$), where Y represents the colorimetric signal on the T line minus the blank control, and X

denotes the thrombin concentration (Figure 2C). For the fluorescence mode, the linear equation was Y = 4189.821X + 4361.261 (R^2 = 0.982), where Y represents the fluorescence signal on the T line minus the blank control, and X is the logarithm of the thrombin concentration (Figure 2D). Both equations demonstrated strong linearity, confirming the high detection performance of the dual-mode FRET lateral flow strip.

To further validate the catalytic activity of AuNPs captured on the T-line of the LFS and enable electrochemical quantification of thrombin, the T-line segments were excised after the reaction and immersed in a redox solution containing 5 mM $K_3[Fe(CN)_6]$, 5 mM AB ($H_3N–BH_3$), and 10 mM PBS (pH 7.4). In the presence of AuNPs, Fe^{3+} was catalytically reduced to Fe^{2+} by AB, generating measurable electrochemical signals. Figure 3A depicts the AuNP-mediated redox reaction at the T-line of the LFS, which was completed within 2 min. As shown in Figure 3B, the electrochemical response exhibited a clear, concentration-dependent increase in current intensity with rising thrombin concentrations, confirming the platform's high sensitivity and quantitative detection capability. These findings further expand the detection capabilities of the dual-mode FRET-LFS system.

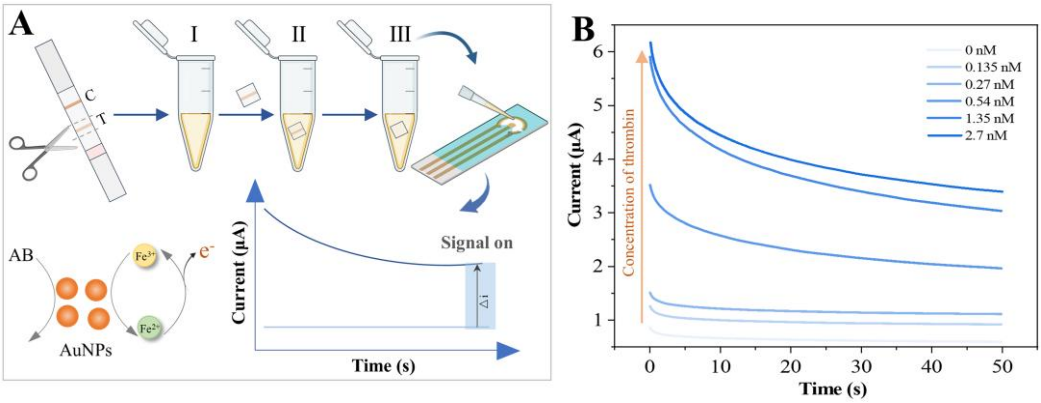

Figure 3. (**A**) Schematic illustration of the AuNP-mediated redox reaction at the T-line of the LFS, with the resulting signal detected by electrochemical measurement. Step I: Preloaded redox solution composed of 5 mM $K_3[Fe(CN)_6]$, 5 mM AB ($H_3N–BH_3$), and 10 mM PBS (pH 7.4). Step II: The T-line region of the LFS is excised and incubated in the redox solution for 2 min. Step III: In the presence of AuNPs, Fe^{3+} is catalytically reduced to Fe^{2+} by AB, generating an electrochemical signal. For electrochemical detection, a constant potential of 0.3 V was applied for 50 s. (**B**) The i-t curves of the AuNP-mediated redox reaction in response to target thrombin at varying concentrations were recorded.

3.3. Specificity and Stability Evaluation of the Dual-Mode FRET Lateral Flow Strip

The specificity of the dual-mode FRET lateral flow strip was assessed using common interfering proteins that could potentially affect the reliability of related protocols in practical applications. Various interfering proteins were tested at concentrations 100 times higher (270 nM) than thrombin (2.7 nM), and the results were compared with those obtained for thrombin. As expected, only the sample containing thrombin generated a colorimetric signal, while samples with other interfering proteins produced results consistent with the blank control (Figure 4A). Notably, fluorescence signal analysis of the T-line followed an opposite trend to the colorimetric signal, also showing specificity in thrombin detection. Specifically, only thrombin, the target analyte, induced the formation of the sandwich structure, leading to fluorescence quenching on the T line (Figure 4B). The corresponding peak intensity variations on the T line are shown in Figure 4C,D. Only thrombin induced detectable intensity variations, while control proteins did not, confirming the excellent specificity of the dual-mode FRET lateral flow strip and its potential for practical clinical applications.

In addition to demonstrating high specificity, stability is crucial for ensuring the method's overall reliability and effectiveness. To evaluate this, a batch of dual-mode FRET lateral flow strips was fabricated, sealed, and stored at 25 °C and 45 °C for various durations (0, 3, 6, 9, 12, and 15 days). The stored strips were subsequently used to detect a 1.35 nM thrombin sample. As shown in Figure 5, even after 15 days of storage, both colorimetric and fluorescent signals exhibited only minor variations. The relative standard deviations (RSDs) in colorimetric mode were 8.08% at 25 °C and 11.29% at 45 °C, while those in fluorescent mode were 8.28% and 10.24%, respectively. These results indicate that the dual-mode sensor exhibits good stability under different storage temperatures.

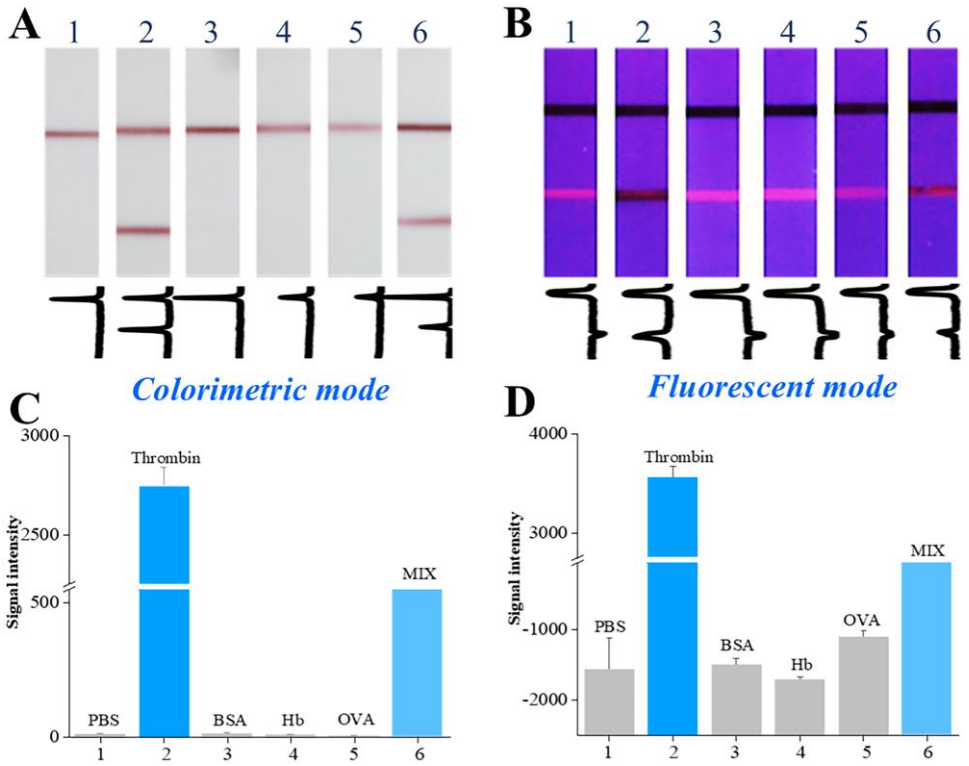

Figure 4. Selectivity evaluation of the colorimetric mode (**A**) and fluorescent mode (**B**) of the FRET lateral flow strip for detecting various proteins and their mixtures. The concentration of non-target proteins is maintained at 270 nM, while the target thrombin concentration is fixed at 2.7 nM. (**C**) Quantification of T-line grayscale values for the FRET lateral flow strip in (**A**). (**D**) Quantification of T-line peak signals for the FRET lateral flow strip in (**B**). BSA: Bovine serum albumin; Hb: Hemoglobin; OVA: Ovalbumin.

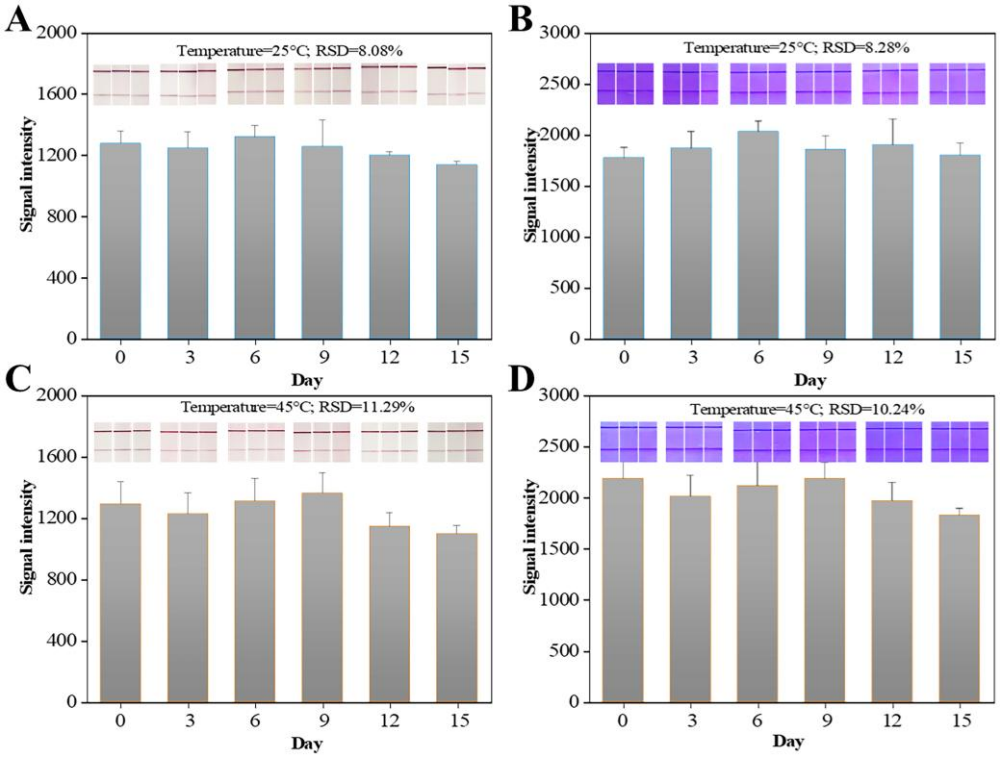

Figure 5. Stability Evaluation of the dual-mode FRET lateral flow strip. The sensors were stored at 25 °C for periods of 0, 3, 6, 9, 12, and 15 days, with measurements taken in both colorimetric mode (**A**) and fluorescent mode (**B**). The same evaluation was performed at 45 °C under the same time intervals, with measurements also taken in colorimetric mode (**C**) and fluorescent mode (**D**).

3.4. Analysis of the Thrombin Detection Performance of the FRET Lateral Flow Strip in Serum Samples

After confirming the high sensitivity and selectivity of the developed biosensor for thrombin detection, we evaluated its performance in real serum samples using the classical spiking method. Thrombin standards at varying concentrations were introduced into blank serum samples and analyzed using the dual-mode FRET lateral flow strip. The detection results exhibited opposite trends under natural and ultraviolet light exposure (Figure 6). A distinct colorimetric signal appeared on the T line at 0.27 nM, whereas significant fluorescence quenching was observed at 0.135 nM under UV illumination. The visual limit of detection (vLOD) for thrombin was 0.27 nM in the colorimetric mode and 0.135 nM in the fluorescence mode, demonstrating that the fluorescence mode was twice as sensitive as the colorimetric mode in serum samples. Compared to previously reported thrombin detection methods, this approach offers superior sensitivity and meets the key requirements for on-site detection. Furthermore, the dual-mode FRET lateral flow strip enables dual-signal calibration, further reinforcing its strong potential for practical applications.

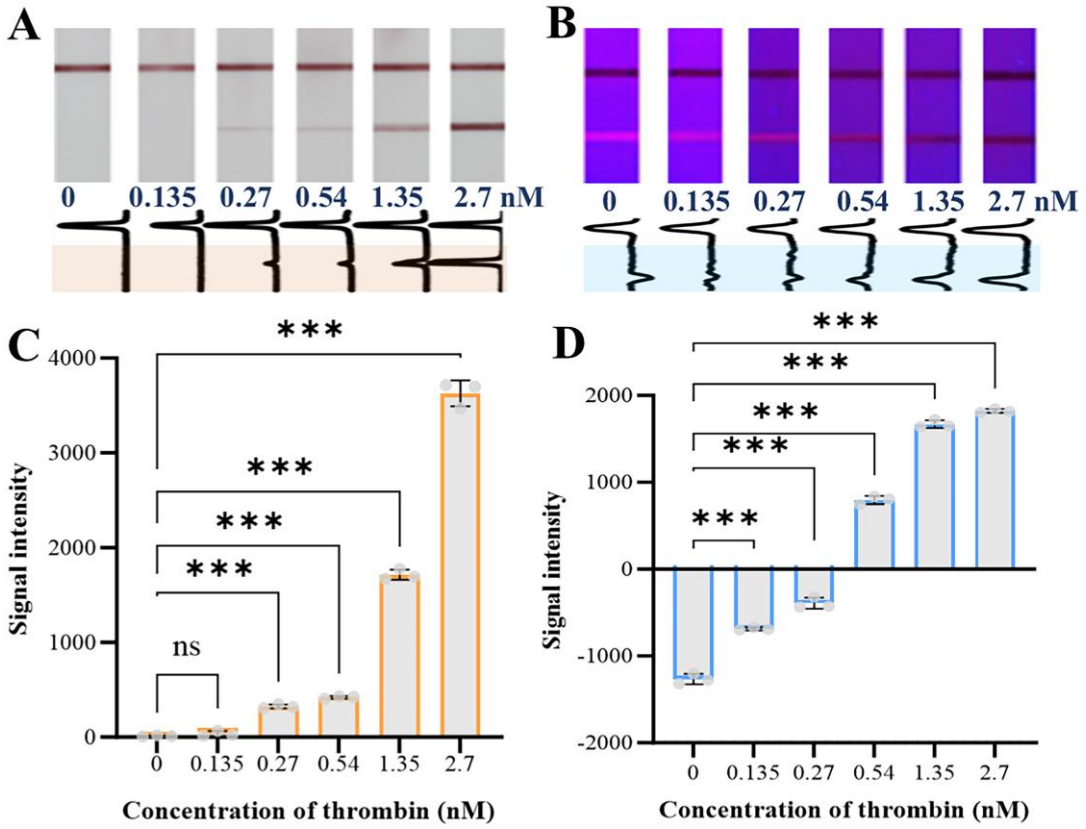

Figure 6. Detection of thrombin in real serum samples using the dual-mode FRET lateral flow strip was performed. The T-line signal intensity was analyzed using one-way analysis of variance (ANOVA). *** $p < 0.001$; ns, not significant. Error bars represent the mean ± SD.

4. Conclusions

In summary, we developed a dual-mode FRET lateral flow strip for the rapid and on-site detection of thrombin, using dual aptamers as recognition probes. This platform integrates the fluorescent properties of QDs with the colorimetric characteristics of AuNPs to establish a highly sensitive FRET-based sensing system. The sensor exhibited excellent performance in detecting thrombin in human serum, generating dual-signal variations in both colorimetric and fluorescent modes. Notably, it enabled rapid and highly sensitive detection, achieving a vLOD of 0.135 nM in fluorescent mode and 0.27 nM in colorimetric mode. The robust FRET protocol enhances reliability and reproducibility, ensuring accurate detection. Additionally, the dual-mode lateral flow strip offers dual calibration, improving detection precision and robustness. Its high accuracy makes it a promising tool for diverse applications, including clinical diagnostics, food safety monitoring, and environmental analysis. Furthermore, the platform exhibits good potential for multiplexing. By integrating multiple aptamer pairs specific to different biomarkers and labeling them with quantum dots of distinct emission wavelengths, it would be feasible to simultaneously detect several targets on a single strip. This capability could be further enhanced by spatially separating detection zones along the strip, enabling parallel analysis with minimal signal interference. Future

advancements may further extend its applicability to the detection of other biomolecules, reinforcing its role as a versatile and reliable platform for sensitive on-site detection.

Author Contributions

Q.C.: methodology, investigation, conceptualization, methodology, software, writing—original draft preparation; L.Y.: methodology, data curation; W.Q.: investigation; H.Y.: investigation, validation; C.Y.: methodology, validation; J.X.: supervision; W.C.: conceptualization, supervision, writing—original draft preparation; writing—reviewing and editing. All authors have read and agreed to the published version of the manuscript.

Funding

This research was funded by the NSFC (32172295), the grants of the Hainan Key Research Program (ZDYF2022XDNY248), the grant of Shanghai S&T Commission (22N31900500), the Anhui Key Research Program (2022k07020009) and the Science & Technology grant of Shihezi, the 8th Division (2023GY02).

Data Availability Statement

Authors ensured that all the data of the study were accessible if required.

Conflicts of Interest

The authors declare no conflict of interest.

References

1. Hattori, M.; Sugiura, N.; Wazawa, T.; et al. Ratiometric Bioluminescent Indicator for a Simple and Rapid Measurement of Thrombin Activity Using a Smartphone. *Anal. Chem.* **2021**, *93*, 13520–13526.
2. Popović, M.; Smiljanić, K.; Dobutović, B.; et al. Thrombin and vascular inflammation. *Mol. Cell. Biochem.* **2012**, *359*, 301–313.
3. Han, C.; Yuan, X.; Shen, Z.; et al. A paper-based lateral flow sensor for the detection of thrombin and its inhibitors. *Anal. Chim. Acta* **2022**, *1205*, 339756.
4. Liu, X.H.; Ba, R.Y.; Wang, W.H.; et al. Roles of nanomaterials in thrombin detection. *TrAC-Trends Anal. Chem.* **2024**, *175*, 117734.
5. Ye, F.; Garton, H.J.L.; Hua, Y.; et al. The Role of Thrombin in Brain Injury After Hemorrhagic and Ischemic Stroke. *Transl. Stroke Res.* **2021**, *12*, 496–511.
6. Liu, Z.W.; Ma, N.; Yu, S.B.; et al. Hemin-catalyzed SI-RAFT polymerization for thrombin detection. *Microchem. J.* **2023**, *189*, 108521.
7. Troisi, R.; Balasco, N.; Autiero, I.; et al. Exosite Binding in Thrombin: A Global Structural/Dynamic Overview of Complexes with Aptamers and Other Ligands. *Int. J. Mol. Sci.* **2021**, *22*, 10803.
8. Ning, J.; Bao, X.; Chen, H.; et al. A highly sensitive and specific fluorescent probe for thrombin detection and high-throughput screening of thrombin inhibitors in complex matrices. *Spectrochim. Acta Part A Mol. Biomol. Spectrosc.* **2025**, *325*, 125136.
9. Samani, S.S.; Sameiyan, E.; Yazdi, F.T.; et al. Sandwich-type aptamer-based biosensors for thrombin detection. *Anal. Methods-UK* **2024**, *16*, 1985–2001.
10. Soni, G.K.; Wangoo, N.; Sharma, R.K. A smartphone-based ultrasensitive colorimetric aptasensing platform for serine protease thrombin detection. *Microchem. J.* **2024**, *199*, 109906.
11. Zhang, J.; Xiang, J.; Liao, L.; et al. Proximity binding-initiated DNA walker and CRISPR/Cas12a reaction for dual signal amplification detection of thrombin. *Talanta* **2023**, *256*, 124286.
12. Huang, Y.; Li, S.; Liu, C.; et al. One-step competitive assay for detection of thrombin via disassembly of diblock oligonucleotide functionalised nanogold aggregates. *Sensor Actuat. B-Chem.* **2023**, *376*, 133032.
13. Sharma, R.; Waller, A.P.; Agrawal, S.; et al. Thrombin-Induced Podocyte Injury Is Protease-Activated Receptor Dependent. *J. Am. Soc. Nephrol.* **2017**, *28*, 2619–2631.
14. Raucci, A.; Sorrentino, G.; Singh, S.; et al. Cost-effective, user-friendly detection and preconcentration of thrombin on a sustainable paper-based electrochemical platform. *Anal. Bioanal. Chem.* **2025**, *417*, 1863–1872.
15. Wang, Y.; Liu, C.; Zhao, W.; et al. Biosensors and Biomarkers for the Detection of Motion Sickness. *Adv. Healthc. Mater.* **2025**, *14*, e2403606.
16. Vairaperumal, T.; Huang, C.C.; Liu, P.Y. Optical Nanobiosensor-Based Point-of-Care Testing for Cardiovascular Disease Biomarkers. *ACS Appl. Bio Mater.* **2023**, *6*, 2591–2613.
17. Dong, T.; Yu, C.; Mao, Q.; et al. Advances in biosensors for major depressive disorder diagnostic biomarkers. *Biosens.*

Bioelectron. **2024**, *258*, 116291.
18. Klebes, A.; Ates, H.C.; Verboket, R.D.; et al. Emerging multianalyte biosensors for the simultaneous detection of protein and nucleic acid biomarkers. *Biosens. Bioelectron.* **2024**, *244*, 115800.
19. Chen, Q.; Yao, L.; Wu, Q.; et al. Rapid and simultaneous visual typing of high-risk HPV-16/18 with use of integrated lateral flow strip platform. *Microchim. Acta* **2022**, *189*, 350.
20. Miller, B.S.; Bezinge, L.; Gliddon, H.D.; et al. Spin-enhanced nanodiamond biosensing for ultrasensitive diagnostics. *Nature* **2020**, *587*, 588–593.
21. Tran, V.; Walkenfort, B.; König, M.; et al. Rapid, quantitative, and ultrasensitive point-of-care testing: A portable SERS reader for lateral flow assays in clinical chemistry. *Angew. Chem. Int. Edgl.* **2019**, *58*, 442–446.
22. Ding, X.; Ma, J.; Fan, T.; et al. Inorganic nanoparticles-based strategies for the microbial detection in infectious diseases. *Interdiscip. Med.* **2024**, *2*, e20230045.
23. Wei, R.; Wang, D.; Zhou, P.; et al. A lateral flow assay strip for simultaneous detection of miRNA and exosomes in liver cancer. *Chem. Commun.* **2024**, *60*, 7491–7494.
24. Wang, Z.; Zhao, J.; Xu, X.; et al. An overview for the nanoparticles-based quantitative lateral flow assay. *Small Methods* **2022**, *6*, 2101143.
25. Su, L.H.; Chen, Y.Q.; Wang, L.L.; et al. Dual-signal based immunoassay for colorimetric and photothermal detection of furazolidone. *Sensor Actuat. B-Chem.* **2021**, *331*, 129431.
26. Sena-Torralba, A.; Torné-Morató, H.; Parolo, C.; et al. A novel ratiometric fluorescent approach for the modulation of the dynamic range of lateral flow immunoassays. *Adv. Mater. Technol.-US* **2022**, *7*, 2101450.
27. Wu, G.; Du, C.; Peng, C.; et al. Machine learning-assisted laccase-like activity nanozyme for intelligently onsite real-time and dynamic analysis of pyrethroid pesticides. *J. Hazard. Mater.* **2024**, *480*, 136015.
28. Liu, X.; Chen, X.; Yin, S.; et al. Dual-modal detection of antimicrobial susceptibility in pathogenic bacteria based on the high-throughput microfluidic platform. *Chem. Eng. J.* **2024**, *499*, 156506.
29. Cao, L.; Ren, Y.; Ling, N.; et al. An ultrasensitive smartphone-assisted bicolor-ratiometric fluorescence sensing platform based on a “noise purifier” for point-of-care testing of pathogenic bacteria in food. *Food Chem.* **2024**, *446*, 138805.
30. Wang, S.; Liang, N.; Hu, X.; et al. Carbon dots and covalent organic frameworks based FRET immunosensor for sensitive detection of Escherichia coli O157:H7. *Food Chem.* **2024**, *447*, 138663.
31. Koo, J.J.; Jung, K.H.; Park, K.; et al. Characterization of the Interfacial Structures of Core/Shell CdSe/ZnS QDs. *J. Phys. Chem. Lett.* **2022**, *13*, 7220–7227.
32. Nie, Y.; Liu, Y.; Zhang, Q.; et al. Fe_3O_4 NP@ZIF-8/MoS_2 QD-based electrochemiluminescence with nanosurface energy transfer strategy for point-of-care determination of ATP. *Anal. Chim. Acta* **2020**, *1127*, 190–197.
33. Lao, X.; Liu, Y.; Li, L.; et al. Plasmon-enhanced FRET biosensor based on Tm^{3+}/Er^{3+} co-doped core-shell upconversion nanoparticles for ultrasensitive virus detection. *Aggregate* **2024**, *5*, e448.
34. Castro, R.C.; Pascoa, R.; Saraiva, M.; et al. Exploring Distinct Second-Order Data Approaches for Thiamine Quantification via Carbon Dot/Silver Nanoparticle FRET Reversion. *Biosensors* **2024**, *14*, 604.
35. Wang, Z.; Xing, K.; Ding, N.; et al. Lateral flow immunoassay based on dual spectral-overlapped fluorescence quenching of polydopamine nanospheres for sensitive detection of sulfamethazine. *J. Hazard. Mater.* **2022**, *423*, 127204.
36. Shan, X.; Lu, J.; Li, C.; et al. Ultrasensitive solid-state electrochemiluminescence sensor based on lotus root shaped carbon fiber, CdSe QDs and Fe_3O_4 synergically amplify Ru (bpy) 32+ luminophore signal for detection of cyfluthrin. *Microchim. Acta* **2024**, *191*, 215.
37. Wang, S.; Zong, Z.; Xu, J.; et al. Recognition-Activated Primer-Mediated Exponential Rolling Circle Amplification for Signal Probe Production and Ultrasensitive Visual Detection of Ochratoxin A with Nucleic Acid Lateral Flow Strips. *Anal. Chem.* **2023**, *95*, 16398–16406.